TABLE I. Wavelength of the maximum of the F, K, and R bands in additively colored KCl.[a]

Temperature °K	K	F	R_1	R_2
18	464 mμ 2.68 ev	533 mμ 2.33 ev	733 mμ 1.70 ev	656 mμ 1.89 ev
83	468 mμ 2.65 ev	537 mμ 2.31 ev	732 mμ 1.70 ev	658 mμ 1.89 ev

[a] Thickness of crystal 0.016 inch.

broadness of the bands may add an uncertainty of approximately 2 mμ, and the measurements certainly cannot be made closer than to 2 or 3 mμ, giving a total uncertainty in the wavelength of roughly 4 mμ. The $K(V_0)$ band measured by Duerig and Markham has a wavelength of 455 mμ or 2.73 ev at a measurement temperature of 5°K.

The ratio of the peak intensity of the F and K bands and its possible variation is also of considerable interest. Table II summarizes the results on these ratios. The

TABLE II. Densities and ratios of densities of F, K, and R bands in KCl measured at 100°K.

No.	Crystal Thickness inch	Optical density F	K	R_1	R_2	F/K	F/R_1	F/R_2	Remarks
1	0.016	2.61	0.44	0.62	0.74	5.9	4.2	3.5	K band resolved
6	0.009	2.57	0.38	0.43	0.43	6.8	6.0	6.0	K band with very
2	0.013	2.04	0.38	0.48	0.55	5.4	4.3	3.7	slight minimum be-
10	0.021	1.98	0.36	0.38	0.43	5.5	5.2	4.6	tween K and F band

crystals were colored and quenched as indicated above, and no subsequent bleaching, heating, or quenching was performed on them. The F/K ratios differ significantly from the x-ray data of Dorendorf and Markham. Seitz[12] gives 21 for this ratio, based on Duerig and Markham's data; Dorendorf's curves give a figure of roughly 13.

I should like to thank Dr. H. Friedman for suggesting a renewed investigation of additively colored alkali halides, and Dr. D. Dexter for several discussions on K centers.

[1] F. G. Kleinschrod, Ann. Physik **27**, 97 (1936).
[2] N. F. Mott and R. W. Gurney, *Electronic Processes in Ionic Crystals* (Oxford University Press, London, 1940), p. 114.
[3] H. Dorendorf, Z. Physik **129**, 166 (1950).
[4] W. H. Duerig and J. J. Markham, Phys. Rev. **88**, 1043 (1952).
[5] Casler, Pringsheim, and Yuster, J. Chem. Phys. **18**, 887 (1950).
[6] H. W. Etzel and F. E. Geiger, Jr., Phys. Rev. **96**, 225 (1954).
[7] H. Pick, Ann. Physik **31**, 365 (1938).
[8] S. Petroff, Z. Physik **127**, 443 (1950).
[9] A. B. Scott and L. P. Bupp, Phys. Rev. **79**, 341 (1950).
[10] R. Kaiser, Z. Physik **132**, 482 (1952).
[11] Both Pick and Petroff heated and then quenched their crystals before measurement, Kleinschrod apparently did not, although this is not explicitly mentioned. Scott and Bupp show F, R_1, R_2, and M bands at 80°K but no K band for a crystal which had not been heated and quenched before the absorption measurement. Kaiser's curves of evaporated KCl taken at 90°K show R and M bands but apparently no K bands.
[12] F. Seitz, Revs. Modern Phys. **26**, 7 (1954).

Upper Limit for the Lifetimes of Excited States of Ni^{60}†

Z. BAY, V. P. HENRI, AND F. MCLERNON
The George Washington University, Washington, D. C.
(Received October 25, 1954)

AN upper limit of 10^{-11} second for the lifetimes of the two excited states of Ni^{60} following the beta decay of Co^{60} has been determined. The E_2 transition energies are 1.17 and 1.33 Mev.

A thin Co^{60} source (~20 microcuries) electrolytically deposited on a Cu disk (440 mg/cm²) is placed between two diphenyl acetylene crystals, called A (8×8×20 mm³) and B (1.5×8×8 mm³), each facing a 1P21 photomultiplier. Between the Co^{60} source and crystal B an Al absorber (98 mg/cm²) can be interposed, preventing any betas from reaching B; betas can never reach crystal A.

With the Al absorber alternatively in and out of place, we measured a $[\gamma_1\gamma_2+\gamma_2\gamma_1]$ coincidence curve, called $[\gamma\gamma]$, and a composite $[\beta\gamma_1+\beta\gamma_2]+[\gamma_1\gamma_2+\gamma_2\gamma_1]$ coincidence curve, called $[\beta\gamma]+[\gamma\gamma]$. The difference between these two curves is the $[\beta\gamma]$ curve. No "prompt" source is needed in this experiment because application of moment theorems[1] to the $[\beta\gamma]$ and $[\gamma\gamma]$ curves yields for the mean lives of the upper (θ_1) and of the lower (θ_2) excited states:

$$\theta_1=(5/4)\Delta\mu_1-\tfrac{1}{4}\{9(\Delta\mu_1)^2-4(\Delta\mu_2-2\mu_1[\gamma\gamma]\Delta\mu_1)\}^{\frac{1}{2}}, \quad (1)$$

and

$$\theta_2=-\tfrac{1}{2}\Delta\mu_1+\tfrac{1}{2}\{9(\Delta\mu_1)^2-4(\Delta\mu_2-2\mu_1[\gamma\gamma]\Delta\mu_1)\}^{\frac{1}{2}}, \quad (2)$$

where $\Delta\mu_n$ is the difference between the nth normalized moments of the $[\beta\gamma]$ and $[\gamma\gamma]$ curve and $\mu_1[\gamma\gamma]$ is the normalized first moment (centroid) of the $[\gamma\gamma]$ curve.

In our coincidence equipment, shown in Fig. 1, the outputs of detectors A and B are branched to the two coincidence circuits C and D. C is a diode bridge coincidence circuit[2] with no variable time delay in its channels. Its resolving time (5×10^{-9} second) is chosen to exceed the two expected lifetimes and all time lags present by at least one order of magnitude. C yields the total coincidence counting rate N_0.[3] D is a differential

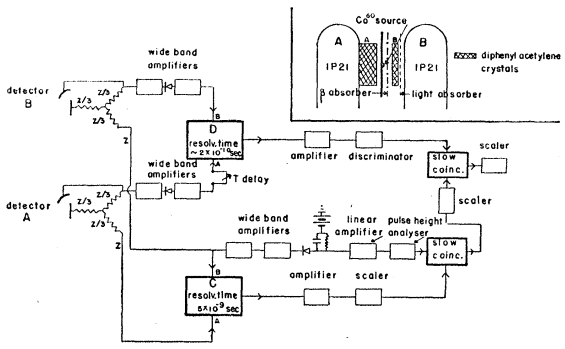

FIG. 1. Schematic diagram of circuits for detecting coincidences.

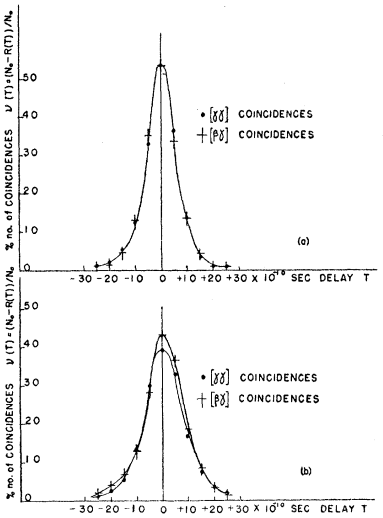

FIG. 2. $[\gamma\gamma]$ and $[\beta\gamma]$ delayed coincidence curves. In Fig. 2a, $[\gamma\gamma]$ and $[\beta\gamma]$ coincidences were selected by use of a pulse height analyzer as described in the text. In Fig. 2b, $[\gamma\gamma]$ coincidences were obtained while using a light absorber between crystal B and its photomultiplier.

coincidence circuit[4–6] with a variable time delay T in its channel A. For coincidences, D gives positive outputs [counting rate $D_+(T)$] if the pulse in channel A arrives later than that in B, negative outputs [counting rate $D_-(T)$] for the opposite case, and no output for the most accurate coincidences occurring. Hewlett Packard 460A amplifiers amplify the D input pulses to be certain that, whenever C detects a coincidence, D has a response. The operation of D is independent of pulse lengths and its resolving time can be as low as 10^{-10} second. Slow coincidences (10^{-5} second) between the outputs of C and D produce a counting rate $R(T)$. Plotting $\nu(T)=[N_0-R(T)]/N_0$ *versus* T, we obtain the "reduced coincidence curves."

From $\nu(T)$ we compute $\bar{t}$, a mean of the random time lags occurring in the equipment.[3,5] A small value of $\bar{t}$ is important for good statistical accuracy of time measurements.[3,7] When the photomultiplier pulses were used without any pulse-shaping, $\bar{t}$ was 8×10^{-10} second. This has been reduced to 4.5×10^{-10} second by a clipping method (anode pulses shortened by dynode pulses).[8] The observed $\bar{t}$ is not far from the theoretical lower limit for the radiations and the detectors used.[9]

In our case, the usual requirement for using the same amplitude distributions to measure two different coincidence curves applies only to channel B, since there is no change in the excitation of channel A for the measurement of the two curves. In order to obtain a pulse height selection, Channel B is branched at the input to C and the branched pulses sent through a diode, followed by an RC circuit (10^{-6} second), to a linear amplifier and then to an Atomic Instrument Company 501 pulse height analyzer. In order not to overload the input of the pulse height analyser, a preselection was performed by biasing the diode. The selected pulses were used to gate (5×10^{-6} second) the outputs of C. About 15 percent of the $[\gamma\gamma]$ and 5 percent of the $[\beta\gamma]$ coincidences were selected.

The curves in Fig. 2a show no difference exceeding statistical fluctuations, thereby indicating very short lifetimes. Therefore, Eqs. (1) and (2) can only be used to set an upper limit for θ_1 and θ_2 giving $\theta_1+\theta_2/2=\Delta\mu_1$ (shift of the centroids).

The curves in Fig. 2a represent one set of measurements corresponding to $\sim$4000 coincidences for each curve. Three such sets gave for the average displacement of the centroids 0.1×10^{-12} second with a maximum deviation of 2.4×10^{-12} second. The calculated statistical error for the entire set of 12 000 coincidences is $\sim1\times10^{-11}$ second. The calculated average difference of times of flight between β's and γ's reaching crystal B (distance from the source = 1.5 mm, crystal thickness = 1.5 mm) is $\sim10^{-12}$ second. Errors due to coincidences resulting from backscattering have been checked and were also found to be negligible. To check our technique for very short time measurements, time-of-flight experiments were performed by varying the position of crystal A. Times of flight as short as a few times 10^{-11} second have been measured and were found to be within the above statistical error, as expected. We consider therefore 10^{-11} second to be the upper limit for the mean lives of both excited states of Ni^{60}. This value is compatible with theoretical estimates.[10,11] (Earlier experiments gave upper limits approximately two orders of magnitude higher.)[12,13]

Next, using Co^{60} as a "prompt" source, we tried to work out a method for similar measurements avoiding use of a pulse height analyser which causes $\sim$90 percent loss of the useful coincidences. We tried to equalize the amplitude distributions for the two radiations by using a light absorber between the crystal and the tube which detect the higher energies of excitation. The decay time of the scintillator is widely independent of energy and (of course) of the number of photons utilized.

First, we determined how the time measurements are influenced by the different β and γ amplitude distributions. Curves 1 and 2 in Fig. 3 show the broad amplitude distributions of β and γ singles in channel B measured in coincidence with the C outputs. The ratio of the average

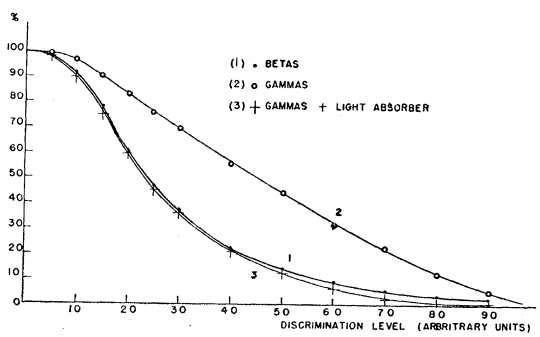

FIG. 3. Integral amplitude distributions of singles in channel B, measured in coincidence with the C outputs.

amplitudes $\bar{A}_\gamma/\bar{A}_\beta$ is 1.6. The shift of the centroids of the corresponding delay curves, taken without pulse height selection, was $(5\pm1)\times10^{-11}$ second.

Using next a light absorber (wire mesh) of the proper transparency between crystal B and its photomultiplier when measuring γ's, it was possible to adjust the γ amplitude distribution to that of the β's so that the rms of the differences between corresponding ordinates was 4.9 percent (curve 3, Fig. 3). The shift of the centroids of the corresponding delay curves (Fig. 2b) was $(0.5\pm1)\times10^{-11}$ second, i.e., within statistical accuracy. From this it appears that the equalization of amplitude distributions to within a few percent, permits one to make time measurements by the coincidence method with an accuracy of $\sim10^{-11}$ second.

† This work was supported by the joint program of the U. S. Office of Naval Research and the U. S. Atomic Energy Commission.

[1] Z. Bay, Phys. Rev. **77**, 419 (1950).
[2] Z. Bay, Rev. Sci. Instr. **22**, 397 (1951).
[3] Bay, Kanner, and Henri, Oak Ridge National Laboratory Technical Report ONR Contract 168(00), September, 1953; and to be published.
[4] Z. Bay, Phys. Rev. **83**, 242 (1951).
[5] Bay, Cleland, and McLernon, Phys. Rev. **87**, 901 (1952).
[6] Bay, Henri, and McLernon (to be published).
[7] Kanner, Bay, and Henri, Phys. Rev. **90**, 371 (1953).
[8] Bay, Henri, and McLernon, Phys. Rev. **90**, 371 (1953).
[9] R. F. Post and L. I. Schiff, Phys. Rev. **80**, 1113 (1950).
[10] V. F. Weisskopf, Phys. Rev. **83**, 1073 (1951).
[11] Aeppli, Frauenfelder, Heer, and Rüetschi, Phys. Rev. **87**, 379 (1952).
[12] M. Deutsch and W. E. Wright, Phys. Rev. **77**, 139 (1950).
[13] Gorodetzki, Knipper, Armbruster, and Gallmann, J. phys. et radium **14**, 550 (1953).

Inelastic Collision Cross Sections at 1.0-, 4.0-, and 4.5-Mev Neutron Energies

J. R. Beyster, R. L. Henkel, and R. A. Nobles
Los Alamos Scientific Laboratory, Los Alamos, New Mexico
(Received November 22, 1954)

In recent years, sphere transmission measurements have been used successfully to determine inelastic collision cross sections.[1–5] In this method the transmission of a spherical shell is measured by surrounding either the neutron detector or the neutron source. To minimize the difficulties caused by the highly anisotropic $T(p,n)He^3$ neutron source used in this experiment, the neutron detector was surrounded instead of the source. The maximum spread in neutron energies was 160 kev for the 1-Mev source and about 70 kev for the 4.0 and 4.5-Mev sources. A high-pressure hydrogen gas proportional counter detected the 1-Mev neutrons. At 4.0 and 4.5 Mev, the neutron detector was a hydrogen recoil scintillation counter consisting of nine spheres of plastic phosphor, 0.100 inch in diameter, separated by quartz to reduce gamma-ray sensitivity.[6] Each detector was positioned at about 30 inches from the tritium gas target in the forward direction. It was operated as a biased neutron detector with about ten energy thresholds allowing ten transmissions to be measured simultaneously. This procedure was adopted to obtain information concerning the energy spectrum of inelastic neutrons produced in the spheres.

When calculating inelastic cross sections from observed sphere transmissions, it is important to consider the probability of multiple neutron scattering. The errors which are made by not considering multiple scattering were not investigated accurately until a few years ago. At that time, Bethe[2–4] proposed a simple and accurate method of evaluating multiple scattering in a spherical geometry which agreed with both experimental observation and detailed Monte Carlo calculations of this effect.

We included the following effects in the numerical analysis of the experimental data: (1) the multiple scattering in the sphere, (2) the relative variation in energy and intensity of neutrons over the solid angle subtended by the sphere, (3) the effect of loss of energy in elastic collisions with resulting reduction in counting sensitivity, and (4) the effect of finite detector size inside the sphere. Corrections due to these effects can be computed using basically the Bethe method of analysis. Since the magnitude of the third correction is large for light elements and the higher energy thresholds, this effect was computed by the Monte Carlo method for increased accuracy. All corrections listed above depend to varying extents on the shape of the elastic scattering angular distributions and on the total neutron cross sections. The known angular distributions at 1 Mev[7] and the recently measured distributions at 4.1 Mev[8] were used. To speed up the numerical analysis the entire computing problem was coded for the Los Alamos Maniac Computer by E. D. Cashwell, C. J. Everett, and J. M. Kister.

The cross sections given in Table I for 1-Mev neutron energy were taken with the proportional counter biased at 750 kev. With the exception of gold and silver, the cross sections are relatively insensitive to the energy threshold of the detector and are probably the entire inelastic collision cross sections. This cross section for

Table I. Inelastic collision cross sections.

Element	1 Mev	4.0 Mev	4.5 Mev
Beryllium		0.62±0.05	
Carbon	−0.09±0.14	0.04±0.08	
Aluminum	0.04±0.08	0.75±0.05	0.72±0.06
Titanium		1.28±0.09	1.16±0.09
Iron	0.41±0.04	1.42±0.07	1.34±0.07
Nickel		1.35±0.09	1.50±0.09
Copper	0.21±0.05	1.60±0.07	1.60±0.06
Zinc	0.10±0.06	1.69±0.06	1.81±0.09
Zirconium		1.56±0.07	1.59±0.09
Silver	1.61±0.16	2.05±0.10	2.02±0.11
Cadmium	0.99±0.06	2.05±0.10	2.12±0.11
Tin	0.07±0.05	2.09±0.10	2.18±0.10
Tungsten		2.58±0.20	2.56±0.20
Gold	1.63±0.10	2.75±0.12	2.69±0.13
Lead	0.23±0.04	1.84±0.08	2.02±0.16
Bismuth	0.12±0.04	1.98±0.10	2.19±0.10